JPE 8-4-2

Hybrid Sensor-less Control of Permanent Magnet Synchronous Motor in Low-speed Region

Yasuhiro Yamamoto[†], Hirohito Funato[*] and Satoshi Ogasawara[**]

[†]Core Technology Department Division, Meidensha Corporation, Japan

[*]Dept. of Electrical and Electronics Engineering, Faculty of Engineering, Utsunomiya University, Japan

[**]Division of Systems Science and Informatics, Hokkaido University, Japan

ABSTRACT

This paper proposes a method of improving the stability in sensor-less control of permanent magnet synchronous motors. The control method for low-speed region is divided into two: One is a high frequency method, which involves a problem of reverse rotation once misdetection of the permanent magnet polarity should occur, and another one is a current drive method, which has a problem that phase and speed oscillations are caused by quick speed changes. Hence, authors propose adoption of the current drive method for the basic control system with added compensation of stabilization by means of the high frequency method. This combination secures stable control with no risk of reversal and less vibration. In addition, authors have also considered a frequency separation filter of a shorter delay time so that current control performance will not lower even when high frequencies are introduced. This filter has achieved simplified compensation using repetitive characteristic through the utilization of the periodicity of high frequency current. Simulation and experiment have been conducted to verify that the stable performance of this system is improved.

Keywords: Permanent magnet synchronous motor, Stabilization control, High frequency, Separation filter

1. Introduction

For sensor-less control of Interior Permanent Magnet Synchronous Motors (IPMSM), the control methods in a low-speed region are divided into two categories. One method is to supply constant amplitude current to the motor to revolve the rotor while forcibly attracting the magnetic poles of the rotor, which we call the current

drive method here. Another method is to inject a high frequency voltage or current into the motor in order to estimate the phase of magnetic poles from the information of the detected high frequency components. Speed detection and vector control have been realized by using such estimated phase [1-4]. We call this technique a high frequency method.

A control system in which the high frequency method is applied can directly estimate the phase of magnetic poles. Use of such estimated phases helps attain stable control with minor phase fluctuations. However, this method has a critical problem: Once the function of polarity estimation should fail to correctly identify the N- and S-poles of the

field magnet, or should it determine the polarity opposite, acceleration in the direction of reverse rotation would arise. The major cause of this phase error is the influence of the dead time. Since current amplitude becomes smaller to near zero, a large distortion occurs in the zero crossing of the multiple-phase current waveforms. This distortion causes disturbance in the phase estimation, likely to fail in the polarity detection. At a start-up stage, another means of measurement is needed to discriminate the N- and S-poles, and normally the characteristic of motor magnetic saturation is used for this purpose. Therefore, the high frequency method cannot be applied to the motors that are designed to have low magnetic saturation [5].

On the other hand, the current drive method is free of reversing problem caused by polarity misdetection because it does not use magnetic pole discrimination. However, it has a problem of stepping out when the motor is overloaded because the allowable load torque is low. In addition, IPMSM is subject to vibration of rotational phase when the speed or the load changes because they do not have any damper winding. In addition, IPMSM without damper windings are subject to vibration of rotational phase when the speed or the load changes. IPMSM is characterized by this weak point of being prone to vibration although they have the advantage of low moment of inertia.

Authors discussed the vibration problem in the current drive method, and as a result, this paper offers a method of additional feedback control to restrain vibration. This vibration restraining control uses phase estimation by the previously mentioned high frequency technique, but it does not directly use the estimated phase for control. The Phase is differentiated, and only the component that is equivalent to the speed vibration is extracted, which is then used only for vibration damping. More specifically, this control method has a strong point that it does not involve the risk of reverse rotation runaway, and it also provides a strong damping effect on vibration.

The high frequency technique requires a filter that splits detected current into high frequency components and other components. However, this filter contains a time delay, and therefore, the response characteristic of the current control system is lowered. As a measure against this weak point, we propose a separation filter that has a shorter

delay time, in which we applied simple learning prediction that uses the high frequency periodicity. At the end, the effect of vibration restraint was evaluated by means of simulation and experiment.

2. The Principle of Proposed Control Method

2.1 Basic current control system

A control block diagram of the entire system is given in Fig. 1. This diagram contains the basic current control system and the stability compensation function by the added high frequency technique. In the current control, two current command components have been entered, including the amplitude $|I_1^*|$ and the frequency ω_1^*. This frequency ω_1^* is integrated to give an angle reference θ_γ, and the current regulator is implemented in a rotating reference frame (γ and δ axes) locked to this angle θ_γ. The reverse rotating conversion and two-phase/three-phase conversion convert the output voltage commands of the current regulator to three-phase voltage in the fixed frame for the PWM. In addition, a coordinate conversion that has a characteristic reversal to the voltage command was applied to the three-phase detected current i_u, i_v, and i_w, which were converted into orthogonal biaxial components i_γ and i_δ.

This current control system should set the sampling period to 250 μs or so to ensure that it is realized by a low-cost CPU. Consequently, the performance of current response will be 500 to 1000 rad/s or so. We adopt a new filter system that can be achieved even at this performance limit in the high frequency technique. The frequency separation filter of the high frequency technique has a feature to deteriorate in the separation characteristic if the input quickly changes. Accordingly, a current command first passes through the rate-of-change limiter, and then it is supplied to the current control.

2.2 Pole estimation using high frequency method

Normal IPMSM has the negative saliency ($L_d < L_q$) in the inductance of d-axis and q-axis. The phase estimation principle of high frequency technique utilizes that the inductance of the magnetic pole axis (d-axis) is the smallest.
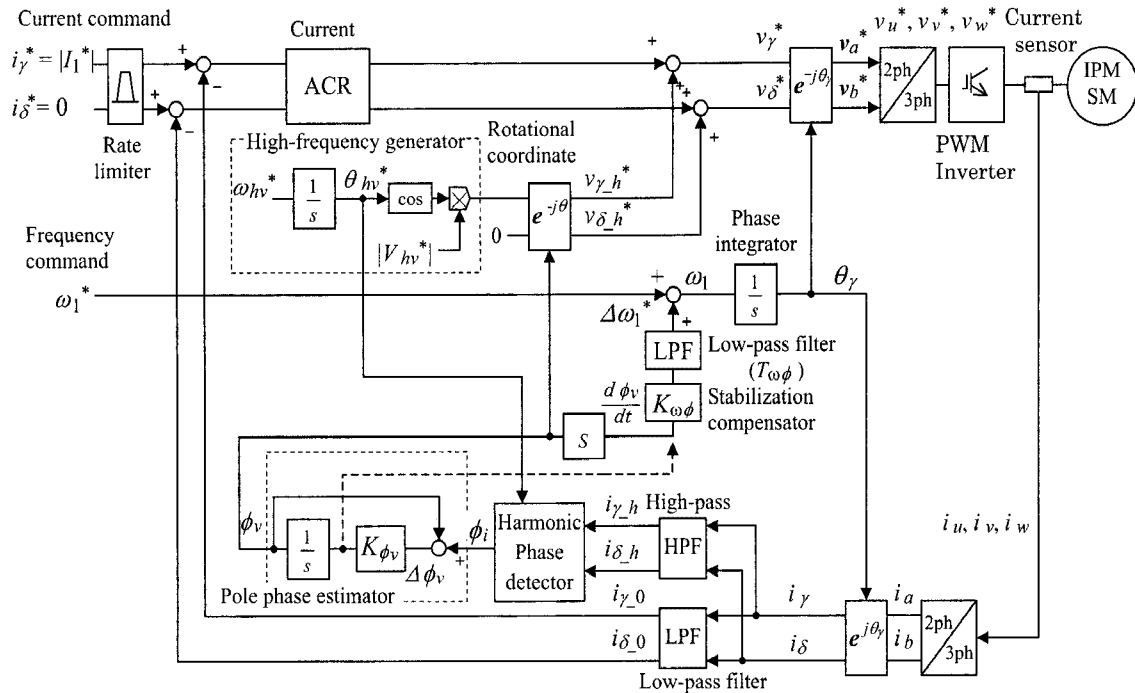
Fig. 1 Control block diagram of proposed

In the case of low current control performance like in this situation, the method of detecting a high frequency current by supplying a high frequency voltage has an advantage in the accuracy. For high frequencies, a simple harmonic motion wave shape is adopted in the input voltage in order to reduce the torque pulsation components due to the high frequency current[1]. Fig. 2 shows the loci of the steady voltage vector v_{1_0}, the steady current vector i_{1_0}, and the high frequency trajectories that superimpose on the former vectors.

This section describes the principle of the magnetic pole phase estimation, which uses high frequency. Fig. 3 shows a diagram in which components are re-plotted so that the centers of high frequency loci of voltage and current will fall on the same point for clearly indicating the phase relation of high frequencies.

High frequency voltage, which is used in this system, supplies eight samples of voltage commands per cycle, with the frequency ω_{hv}^* set to 500 Hz. As shown in Fig. 1, the high frequency command ω_{hv}^* is integrated to calculate the phase θ_{hv}^*, and then a simple harmonic motion voltage command $v_{d\_h}^*$ is generated by the cosine function and the amplitude command $|V_{hv}^*|$. The reference axis θ_γ of current control is offset by ϕ_d from the magnetic pole axis, and
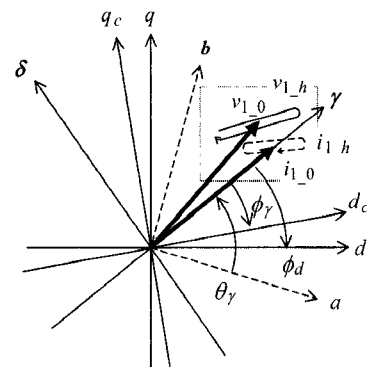

Fig. 2 Definition of the current control coordinates and the magnetic pole coordinates, and loci of the high frequency components
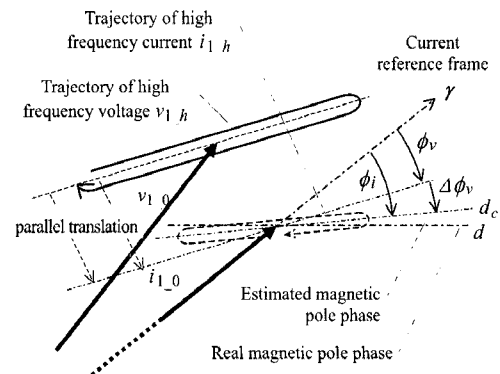

Fig. 3 Injected high-frequency voltage, and pole phase estimated from locus of the detection current

here we assume that this phase offset can be estimated as the offset phase of high frequency voltage axis ϕ_v. The voltage $v_{d\_h}^*$ of d-axis component undergoes rotating coordinates by the degree of this ϕ_v, and it is converted into the components of $v_{\gamma\_h}^*$ and $v_{\delta\_h}^*$ in the γ-δ frame, then they are added to the steady voltage command.

Since the above operation generates a high frequency current, a frequency separation filter is used, which will be described in the next section, to extract the high frequency components from the current detection. Because IPMSM has negative saliency, the phase axis ϕ_i of the high frequency current appears in d-axial direction with smaller inductance from the voltage axis ϕ_v. Use of this feature enables us to find the magnetic pole phase that has the minimum inductance. Specifically, we apply the integral feedback, which can correct the previously mentioned high frequency voltage phase ϕ_v into the direction of the current generation axis ϕ_i. This feedback system leads to a convergence of phase in which the axes of high frequency voltage and high frequency current meet each other, and this is the estimated phase of magnetic pole.

The separation filter of high frequency components i_{γ_h} and i_{δ_h} from the current detection i_γ and i_δ after the coordinate conversion is shown in Fig. 1. Furthermore, in the harmonic phase detection block, the amplitude component of high frequency current $i_{\gamma f}$ and $i_{\delta f}$ is calculated according to the Fourier integral using the phase θ_{hv}^* that is used in generation of the voltage command. Then, the amplitude of these two axes causes the high frequency current axis phase ϕ_i by means of the arctangent function. Since the phase of high frequency current generation has been detected in the above manner, the phase ϕ_v can be corrected by means of integration of the phase difference $\Delta\phi_v$ between the voltage phase ϕ_v and the current phase ϕ_i. Consequently, when the phase difference $\Delta\phi_v$ is converged on zero as previously mentioned, ϕ_v means the pole phase ϕ_d of either the N-pole or the S-pole.

2.3 Stabilization control

Because the pole phase ϕ_d can be estimated, it is possible to apply the compensation that corrects the reference phase θ_γ of the current control in proportion to

ϕ_v, in order to restrain the speed vibration. This is constituted by the components of a pole phase estimator, a differentiation, a stabilization compensator, and a low-pass filter in Fig. 1.

Since distinction of the N-pole and the S-pole is not performed, an error of 180 degrees may be involved in the estimated pole phase. In order to eliminate the effects of this error, only a changed component has to be taken out from the estimated phase. Therefore, the compensator needs to differentiate the estimated phase once, and to integrate it in order to return to the phase component.

In practice, however, signals can be extracted at the point before the integrator ϕ_v to obtain the differential components, just as the route given by broken lines in Fig. 1. The integration can use the section of conversion from speed to phase, by adding the compensation speed $\Delta\omega_1^*$ to the speed command ω_1^*. Use of this configuration does not require any other special differentiation or integration.

2.4 High frequency separation filter

The current drive method requires a moderate level of current control performance for prevention of the current from fluctuation affected by speed changes. However, a delay time will take place if a low pass filter is used to eliminate high frequency components. The current control gain has to be reduced by such a delay time. Therefore, the simplified repetitive compensation that utilizes the periodicity of high-frequency components is applied to the filter. The structure of this frequency separation filter is shown in Fig. 4, and the operation time chart in Fig. 5. The structure in Fig. 4 is expressed in a discrete system that uses a delay operator z^{-1}, consisting of the following three elements.

First, the current detector samples the eight point data $i_\gamma[n]$, which correspond to one cycle, and calculate the moving average thereof. This moving average eliminates the high-pass components, and outputs the average value $ave(i_\gamma[n]: i_\gamma[n-7])$, as given in Fig. 5. However, the outputs contain the detection delay, therefore it cannot be used for current control. Next, the $i_{\gamma\_h}[n]$ is calculated based on the difference between the present value $i_\gamma[n]$ and the moving average $ave(i_\gamma[n]: i_\gamma[n-7])$. It is supplied to the stabilization control as the high-pass components of filter,
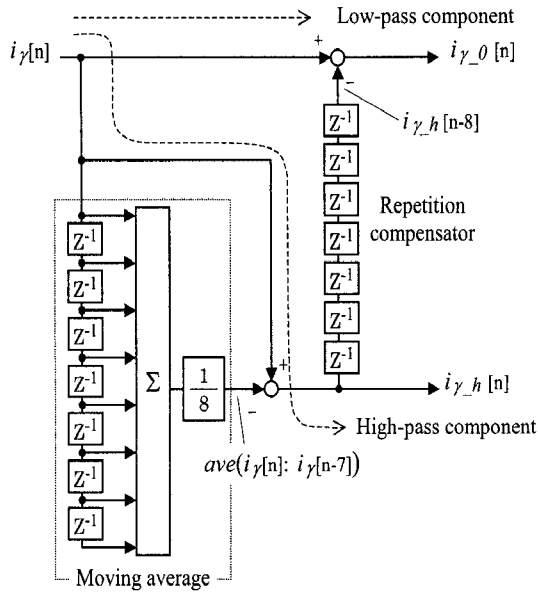
Fig. 4 Separation filter of high and low frequency
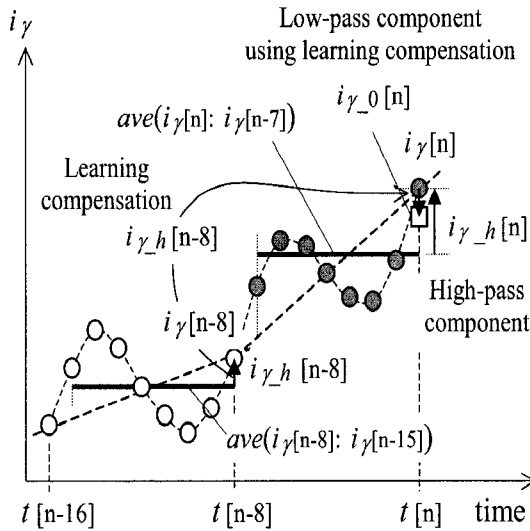component with repetitive compensation

Fig. 5 Timing chart for principle description of high frequency
separation using repetitive characteristics

and at the same time, the value is saved internally for the coming compensation. Eventually, the component without the delay used in current control can be obtained by the following approach. Since the high-frequency components have periodicity, we assume that $i_{\gamma\_h}[n-8]$, in which eight samples of the present detected values $i_{\gamma\_h}[n]$ are stored, can be an approximation of the present high-frequency

component. The present detected value $i_\gamma[n]$, from which $i_{\gamma\_h}[n-8]$ is subtracted, outputs $i_{\gamma\_0}[n]$ from which high-frequency components have been eliminated, as shown in Fig. 5. This low-pass component is used in the current control.

As shown by the route given by broken lines in Fig. 4, both the high frequency components and the high frequency-eliminated components do not pass through the delay operator, which reveals that the separation filter has no time delay.

3. Evaluation of Transient Characteristics

3.1 Evaluation by simulation

The effect of using this system was evaluated by means of simulation and experiment. The parameters of the motor and the control gains are listed in TABLE 1. In the simulation and experiment, the moment of inertia of the motor alone is used so that the vibration frequency will be the highest.

At first, the characteristic of frequency separation filter of current was examined, and the results are shown in Fig. 6. The amplitude of high frequency current was set to approximately 5%, and then, the separation characteristics were checked when the γ-axis current command i_γ^* was changed from 0 to 50%.

Table 1 Motor Parameters and Control Gain for
Experiments

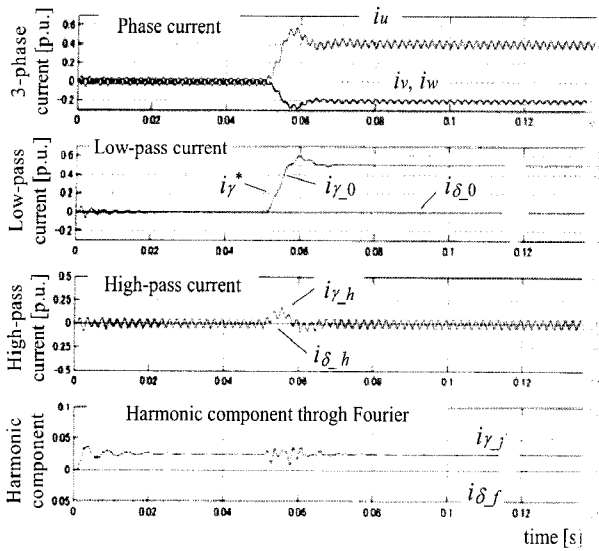| Parameter	Value
Power	37 kW
Pole	6 pole
Rated speed	3400 min⁻¹
Rated voltage	340 V
Rated Current	78 A
Resistance	28 mΩ
Inductance Ld	0.8 mH
Lq	2.4 mH
Moment of Inertia	0.029 kg-m2
Control Gain	$K\phi v = 0.0083$ p.u. $K\omega\phi = 5.7$ p.u./rad $T\omega\phi = 0.01$ s

Fig. 6   Separation characteristics of detection current to high
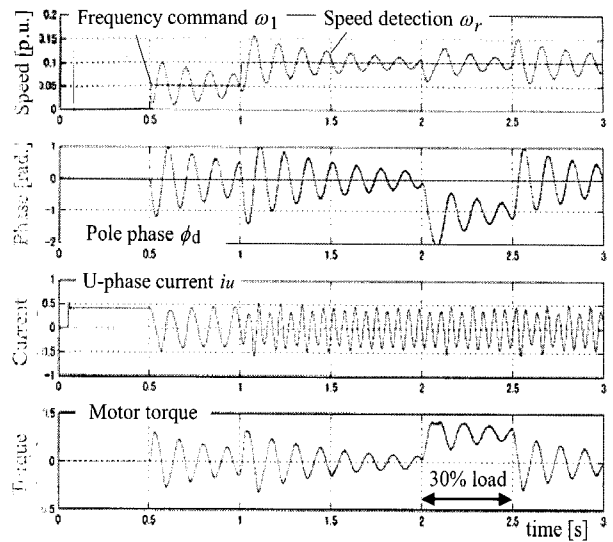frequency and fundamental component

Fig. 7   Unstable characteristics without Stabilization
compensator by Simulation
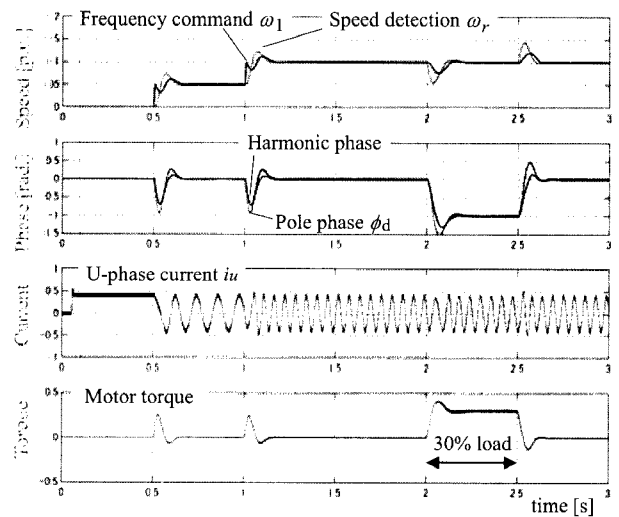
Fig. 8   Transient stability characteristics with proposed
stabilization compensator by Simulation

Since the separation characteristic of this filter deteriorates if there is any discontinuity, a rate-of-change limit of 100% per 10 ms or so is applied to the current command. The current control response was set to approximately 700 rad/s. The three-phase currents i_u, i_v, and i_w containing high frequencies were separated into each component of i_{γ_0} and i_{γ_h} by means of coordinate conversion and the separation filter. Here, the δ components (i_{δ_0}, i_{δ_h}) is zero because of the no load condition ($\phi_v = 0$). From this result, we confirmed that the separation characteristic of the filter is good and the delay time is short. Although DC components are generated in the high-pass current i_{γ_h} when the current changes, but the fundamental harmonic component $i_{\delta f}$ converted using Fourier integral did not find any influence. In other words, it is considered that little effects are seen on the high frequency current phase ϕ_i.

Comparison of vibration restraint effects is shown in Fig. 7 and Fig. 8. Control gains were set as described below. If we combine integrate and feedback, an equivalent low-pass filter results. Since the vibration frequency is about 7 Hz or so in our experiment, $K_{\phi v}$ was set so that a time constant will be 30 ms or so, which is a little longer than this time constant. The control gain $K_{\omega i}$ is a parameter of importance in the stability, and its value was adjusted so that vibration will be smaller in one experiment. $T_{\omega\phi}$ was set to 10 ms so that it will restrain the

residual ripple components of high frequency filter output.

Regarding the running conditions, we assume that the moment of inertia of load is small. The amplitude of current command i_γ^* is set to 50%. At two time points of 0.5 s and 1.0 s, the speed command was increased by 5%. Here, the speed command is subjected to the rate-of-change limit of 100% per 0.1 s. During the period from 2.0 s to 2.5 s, a step load torque of 30% is imposed. Fig. 7 shows that the actual speed and the actual phase are vibrating, and the current amplitude is also distorted affected by the electromotive force.

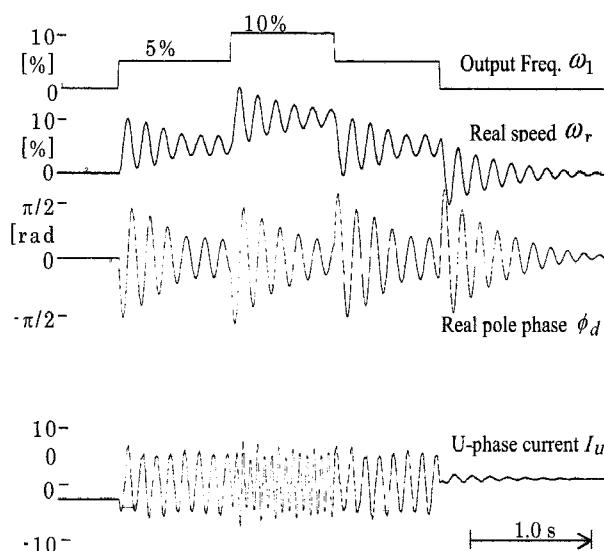In contrast with the above, the application of vibration

Fig. 9   Experimental result of transient characteristics without stability compensation

Fig. 10   Experimental result of transient characteristics with stability compensation

restraint triggers a correction so that the output frequency ω_1 will follow the actual speed ω_r, when the speed command fluctuates, as shown in Fig. 8. This correction can restrain the amount of overshoot of actual speed, offering much more high-speed damping characteristics. When load fluctuation occurs, the degree of speed lowering becomes larger contrariwise to secure stability, but the characteristic of quickly damping the vibration is still offered.

3.2 Evaluation by experiment

To verify the effects of simulation, acceleration and deceleration test was performed using an actual system. To detect the real phase and speed, position sensor was mounted on the motor. With the motor kept running alone, the speed and the phase fluctuation were measured while quickly changing the speed command because the condition for motor alone was the highest vibration frequency. The speed command was changed by three levels of 0%, 5% and 10%, and the rate-of-change limit of speed command were set to the same as in the simulation.

Fig. 9 shows the characteristics of the conventional current drive method, which does not apply any vibration restraint. This diagram indicates that vibration is occurring in the real speed and the real phase, which is similar to the simulation. Fig. 10 shows the characteristics of a case with added vibration restraint control by the high frequency technique. It is shown that the stability is improved, too,
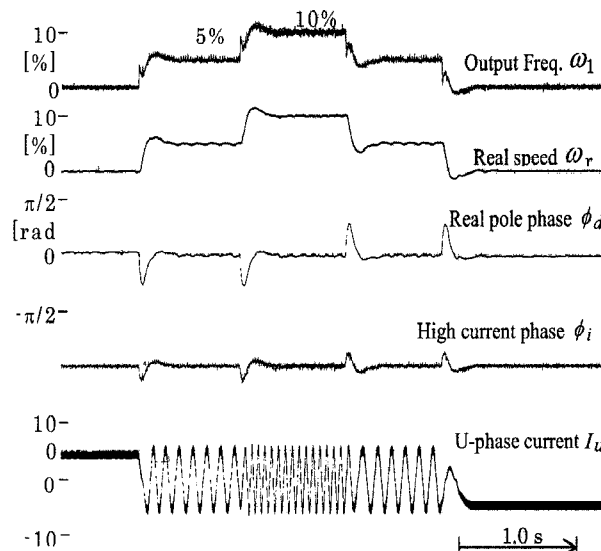
similar to the simulation.

The above results of experiment have confirmed that our proposed method is effective.

4. Conclusions

Our study used the hybrid control, which combined the high frequency technique with the current drive method, and improved the stability. The key is to restrain speed vibration by utilizing the changing portion of the d-axis phase, without performing estimation of the N-pole and the S-pole. For this reason, our system can be applied to the motors that do not have any magnetic saturation characteristic.

Although this method has some shortcomings such as the small startup torque and the tendency of stepping out when overloaded, the method can be applied to a wide variety of motors. The position sensor-less control of IPMSM is limited in its possible applications because the contents of motor design affect the control performance. We expect that our suggestion may help users apply the sensor-less control to much more motors.

References

[1]   T. Aihara, A. Toba, T. Yanase, "Sensor-less Torque Control of Salient-Pole Synchronous Motor at Zero Speed Operation", *the 1996 Japan Industry Applications Society*

　　　　Journal of Power Electronics, Vol. 8, No. 4, October 2008

Conference, No. 170, pp.1-2, 1996.

[2] P. L. Jansen, R. D. Lorenz, "Transducerless position and velocity estimation in induction and salient AC machines", *IEEE Trans. Industry Application*, Vol. 31, No. 2, pp. 1162-1169, March/April 1995.

[3] M. Schroedl, "Sensorless control of AC machines at low speed and standstill based on the 'INFORM' method", *Conf. Rec. of IEEE IAS. Annual Meeting*, pp. 270-277, Oct. 1996.

[4] S. Ogasawara, H. Akagi, "An approach to real-time position estimation at zero and low speed for PM motor based on saliency", *in Proc. IEEE Ind. Appl. Soc. Annual Meeting*, San Diego, CA, pp.29-35, Oct. 5-10, 1996.

[5] N. Bianchi, S. Bolognani, "Influence of Rotor Geometry of an IPM Motor on Sensorless Control Feasibility", *IEEE Trans. Industry Application*, Vol. 43, No. 1, pp. 87-96, 2007.

Yasuhiro Yamamoto was born in Hiroshima Prefecture, Japan in 1958. He received the B.S. and M.S. degrees in electrical engineering from Nagaoka University of Technology, Japan, in 1981, 1983, respectively. Since 1983, he joined Meidensha Corporation, Tokyo, Japan, where he is currently a Senior Engineer. He is in a doctoral program of Utsunomiya University for adult students from 2006. His research interests are the controls of ac motors. Mr. Yamamoto is a Member of the Institute of Electrical Engineers of Japan, IEEE PELS, IEEE IAS.

Hirohito Funato was born on Feb. 26th 1964 in Fukushima, Japan. He received B.E., M.E. and Ph.D. degrees in electrical engineering from Yokohama National University, Japan in 1987, 1989, 1995 respectively. He worked at Tokyo Electric Power Company from 1989 to 1991. He joined the faculty of engineering, Utsunomiya University in 1995 where he is now an associate professor. His research fields include application of power electronics to power system, digital control of power converters, renewable energy and so on. He received the ICPE 2007 Best Paper Award, the PCC 2007 Best Paper Award and the IEEJ Paper Presentation Awards in 1994 and 1997. Dr. Funato is a member of the Institute of Electrical Engineers of Japan, IEEE PELS, IEEE IAS, IEEE IES.

Satoshi Ogasawara was born in Kagawa Prefecture, Japan, in 1958. He received the B.S., M.S., and Dr. Eng. degrees in electrical engineering from Nagaoka University of Technology, Niigata, Japan, in 1981, 1983, and 1990, respectively. From 1983 to 1992, he was a Research Associate with Nagaoka University of Technology. From 1992 to 2003, he has with the Department of Electrical Engineering, Okayama University, Okayama, Japan. From 2003 to 2007, he was with the Department of Electrical Engineering, Utsunomiya University, Utsunomiya, Japan. Since 2007, he has been a Professor in Graduate School of Information Science and Technology, Hokkaido University, Sapporo, Japan. His research interests are ac motor drive systems and static power converters. Dr. Ogasawara received the IEEE/PELS Society Prize Paper Award in 1999, and the IEEE/IAS Committee Prize Paper Awards in 1996, 1997 and 2003. He is a Senior Member of the Institute of Electrical and Electronics Engineers.